Analysis on Local and Concurrent Commutation Failure of Multi-infeed HVDC Considering Inter-converter Interaction

Bilawal Rehman, Chongru Liu, Huan Li, Chuang Fu, and Wei Wei

***Abstract*—This paper provides a comprehensive analysis of local and concurrent commutation failure (CF) of multi-infeed high-voltage direct current (HVDC) system considering multi-infeed interaction factor (MIIF). The literature indicates that the local CF is not influenced by MIIF, whereas this paper concludes that both the local CF and concurrent CF are influenced by MIIF. The ability of remote converter to work under reduced reactive power enables its feature to support local converter via inter-connection link. The MIIF measures the strength of electrical connectivity between converters. Higher MIIF gives a clearer path to remote converter to support local converter, but at the same time, it provides an easy path to local converter to disturb remote converter under local fault. The presence of nearby converter increases the local commutation failure immunity index (CFII) while reducing concurrent CFII. Higher MIIF causes reactive power support to flow from remote converter to local converter, which reduces the chances of CF. A mathematical approximation to calculate the increase in local CFII for multi-infeed HVDC configurations is also proposed. A power flow approach is used to model the relation between MIIF and reactive power support from remote end. The local and concurrent CFIIs are found to be inverse to each other over MIIF; therefore, it is recommended that there is an optimal value of MIIF for all converters in close electric proximity to maintain CFII at a certain level. The numerical results of established model are compared with PSCAD/EMTDC simulations. The simulation results show the details of the influence of MIIF on local CF and concurrent CF of multi-infeed HVDC, which validates the analysis presented.**

***Index Terms*—Commutation failure (CF), multi-infeed high-voltage direct current (HVDC) system, multi-infeed interaction factor, commutation failure immunity index (CFII).**

I. Introduction

MULTI-INFEED direct current (DC) systems are widely found in modern power systems, especially in China [1]. To integrate high power with remote grid, high-voltage direct current (HVDC) system has now become a most economic and reliable candidate due to its capacity of handling and controlling high power. The multi-infeed scenario consists of several HVDC converters in close electric proximity [2]. The multi-infeed HVDC system mostly contains more than one inverter connected to a common alternating current (AC) bus or buses which are close to each other. The fundamentals of four interaction phenomena, i. e., transient over-voltage, commutation failure (CF), harmonics, and voltage/power instability, are discussed in CIGRE report [3]. Among them, the CF for multi-infeed configuration is of the most importance.

The CF in line commutated converter (LCC)-HVDC system is one of the most frequent and adverse phenomena in DC power transfer, especially for inverters in close proximity. The inter-converter interaction has made CF more deteriorative than single-infeed HVDC. The CF on one converter may cause CF on other converters or even all remote converters (concurrent CF) in proximity due to the inter-converter interaction, which could interrupt the HVDC link temporarily or permanently depending upon the fault severity. A typical practice example is the blocking of an HVDC link that caused a power reduction of 4530 MW [4], which happened in 2013 in China, where a converter station was blocked due to concurrent CF.

The commutation failure immunity index (CFII) [5] is a key parameter to evaluate the CF susceptibility of HVDC link. The index was initially proposed for single-infeed HVDC, which is also valid for multi-infeed HVDC system. The CFII can be significantly increased by improving the voltage profile of converter bus [6]. The absence of reactive power support during fault makes the system more prone to risky conditions. To quantify the interaction between converters in multi-infeed configuration, an index called multi-infeed interaction factor (MIIF) [3], [7] is presented, which provides a degree of closeness between two converters of multi-infeed scheme. The value of MIIF always lies between 0 and 1. If the value is 0, it means the two converter buses are infinitely far apart; and if the value is 1, it means both converters are connected to the same AC bus. Particularly,

Manuscript received: April 6, 2020; revised: October 7, 2020; accepted: May 8, 2021. Date of CrossCheck: May 8, 2021. Date of online publication: June 22, 2021.

This work was supported by science and technology project of China Southern Power Grid (No. ZBKJXM20180104).

B. Rehman (corresponding author) and C. Liu are with the State Key Laboratory for Alternate Electrical Power System with Renewable Energy Sources, North China Electric Power University, Beijing 102206, China, and B. Rehman is also with the Department of Electrical Engineering Technology, National Skills University Islamabad, Islamabad, 45710, Pakistan (e-mail: bilawal@nsu.edu.pk; chongru.liu@ncepu.edu.cn).

H. Li, C. Fu, and W. Wei are with the State Key Laboratory of HVDC, Electric Power Research Institute, China Southern Power Grid, Guangzhou 510663, China (e-mail: lihuan3@csg.cn; fuchuang@csg.cn; weiwei@csg.cn).

DOI: 10.35833/MPCE.2020.000164

the occurrence of concurrent CF is coupled with MIIF.

Only a small amount of available literature deals with CF in multi-infeed HVDC systems. The concurrent CFII (C-CFII) is effected by three factors: local AC system strength, remote AC system strength, and MIIF [5]. Local AC system strength influences the C-CFII almost linearly [8]. Higher MIIF causes lower CFII [9]. The analysis concludes that the local CFII (L-CFII) only depends on local AC system strength, while the influence of MIIF is ignored considering local single-infeed HVDC system [10], or the MIIF is considered as constant [11]. However, the assumption of constant MIIF for L-CFII might lead to pessimistic results [12]. To indicate this phenomenon, a detailed analysis on the influence of MIIF on local CF for inverter-rectifier dual infeed HVDC scenario is proposed in [12].

However, the role of MIIF for the inverter-inverter scenario is not declared clearly yet. The impact of MIIF on local CF needs to be carefully investigated for the inverter-inverter scenario, which is more common than the inverter-rectifier scenario. Furthermore, the available literature provides an empirical information about MIIF without giving a mathematical relation between MIIF and inter-converter impedance in case of concurrent CF. In this paper, it has been found that both local CF and concurrent CF are influenced by MIIF. In fact, it is found that L-CFII can be improved with MIIF. A mathematical equation describing MIIF and inter-converter impedance is formulated using power flow approach. Subsequently, an equation is formed to estimate the increase in L-CFII in multi-infeed HVDC system.

The remainder of this paper is organized as follows. Section II briefly describes the indices to measure the risk of CF. Section III explains the influence of MIIF on local CF and concurrent CF. A detailed analysis is carried out to provide significant information about local CF with MIIF. Various practical scenarios are also investigated with and without reactive power support. Section IV presents the mathematical modeling of power flow and provides a relation of MIIF and inter-converter impedance. A mathematical estimation of increase in L-CFII is formulated. Section V verifies the estimated equations and Section VI provides a conclusion.

II. Indices to Measure Risk of CF

CF is an adverse event in successful power transfer via LCC HVDC system. The phenomenon occurs when a converter valve fails to turn off and continues its operation. It mostly happens because of the voltage reduction of commutation bus due to the faults on the AC side. The other reasons include increased DC current, AC voltage phase shift, and AC-side harmonics [13]. The CF probability of LCC-HVDC system can be reduced by improving the voltage profile of commutation bus through installing dynamic reactive power support at an additional cost [14]. Once the CF takes place, it temporarily drops power transfer and increases direct current, which consequently increases stress on the converter valves [15], [16]. On the other hand, the converter absorbs a large amount of reactive power from the AC system during CF. If reactive power support is insufficient, the bus voltage would be further depressed, which increases the risk of continuous CF. Practically, the CF occurs when the inverter's extinction angle γ is less than γ_o [17], where γ_o is critical extinction angle. Typically, the value of γ_o is about 8°. The probability of CF at converter depends on the fault severity, reactive power support, AC system strength, and interaction between converters.

CF is categorized into two types, i.e., local CF and concurrent CF. Local CF is referred to a CF at converter i due to the fault at the bus of converter i (i.e., its own bus), while a concurrent CF is referred to a CF at converter j caused by a fault at the bus of converter i.

Several well-known indices will be used in the rest part of this paper. To better understand the analysis of this paper, they are listed and explained as follows.

1) CFII: the ability of a converter to work normally under severe fault is called its immunity to CF, calculated in (1). The higher the value of CFII is, the more immune it is to the CF (less susceptible).

$$CFII_i = \frac{S_{wf,i}}{P_{dc,i}} \times 100 \tag{1}$$

where S_{wf} is the worst fault apparent power in MVA; P_{dc} is the rated power of converter; and subscript i represents the i^{th} converter.

The CFII denotes the critical fault under which the probability of CF occurrence is 0. If the fault above critical level occurs, it may or may not cause CF. This is due to the fact that CF not only is the function of fault severity, but also depends on time instant at which the fault is induced [18]. Practically, a thyristor requires a turn-off time of approximately 400-500 μs for 50 Hz system, which corresponds to the commutation between valves. If the minimum turn-off time is assumed (i. e., 400 μs), then a complete cycle (20 ms) is divided into 50 equal time intervals and a specified fault is applied at each instant. The fraction of time spans for which CF occurs is called CF probability. Each converter in close proximity has local and concurrent CF immunity and probability.

2) MIIF: MIIF is a measure of closeness between two converters. $MIIF_{21}$ (converter 1 to converter 2) can be calculated as (2) and it is basically the ratio of AC voltage drop at converter 2 (ΔV_2) to that of converter 1 (ΔV_1) followed by a balanced three-phase inductive fault that occurs at converter 1, which produces 1% AC voltage drop at commutation bus 1 [5].

$$MIIF_{21} = \frac{\Delta V_2}{\Delta V_1} \tag{2}$$

3) Short-circuit ratio (SCR) and effective short-circuit ratio (ESCR): SCR can be defined as (3), which is a ratio of short-circuit level (SCL) at converter bus to the rated DC power of the converter [19]. To overcome the impact of the filter on fundamental frequency, ESCR is introduced, which can be calculated as (4) [19].

$$\begin{cases} SCR_i = \dfrac{SCL_i}{P_{dc,i}} \\ SCL_i = \left.\dfrac{V_{th}^2}{Z_{th}}\right|_i \end{cases} \tag{3}$$

$$ESCR_i = \frac{SCL_i - Q_{c,i}}{P_{dc,i}} \quad (4)$$

where Q_c is the reactive power of installed filters and capacitor banks [20]; and V_{th} and Z_{th} are the AC Thevenin voltage and impedance as seen from converter bus, respectively.

III. Influence of MIIF on Local and Concurrent CF in Multi-infeed HVDC

A. CF of Single-infeed HVDC

A 1000 MW 500 kV CIGRE single-infeed benchmark model with SCR of 2.5 is observed under CF, and the results are shown in Fig. 1. The CFII is investigated and found to be 13.5% of SCL.

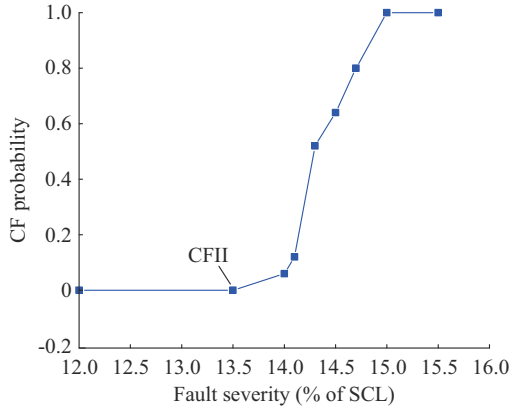

Fig. 1. CF probability of CIGRE benchmark model.

The CIGRE monopolar HVDC benchmark needs reactive power support of approximately 550 Mvar for the rated power operation (1000 MW), as shown in Fig. 2(a). During a fault at the converter bus, the reactive power demand increases in order to operate uninterruptedly. Figure 2(a) also shows the demand of reactive power with fault severity. The range *a* in Fig. 2(a) shows normal operation, *b* denotes the operation under 10% fault severity (i. e., 10% of SCL), *c* shows reactive power required under 13.5% fault severity (135 Mvar), and *d* corresponds to operation under 15% fault severity.

As the CFII of CIGRE benchmark model is 13.5%, the model can operate under a fault of 135 Mvar (*c*) without a CF. This implies that the model has the ability to operate with $Q = (550 - 135)\,\text{Mvar} = 415$ Mvar and $P = 770$ MW as no additional reactive power support is provided for the rated operation as in Fig. 2(b).

In Fig. 2(b), the simulation in PSCAD/EMTDC for CIGRE benchmark model is performed for the above ranges *c* and *d*. *c* shows the operation at 13.5% fault severity, which does not cause CF; and *d* corresponds to CF at 15% fault severity, which produces a net reactive power less than 415 Mvar. Thus, the fault which causes net reactive power $Q_{rated} - Q_{fault}$ less than 415 Mvar may cause CF; and a 135 Mvar is readily available at the inverter station for possible use without severe harm (i. e., CF) to the operation of inverter. This ability of the inverter to operate under reduced reactive power is beneficial for remote converter in multi-infeed scenario.

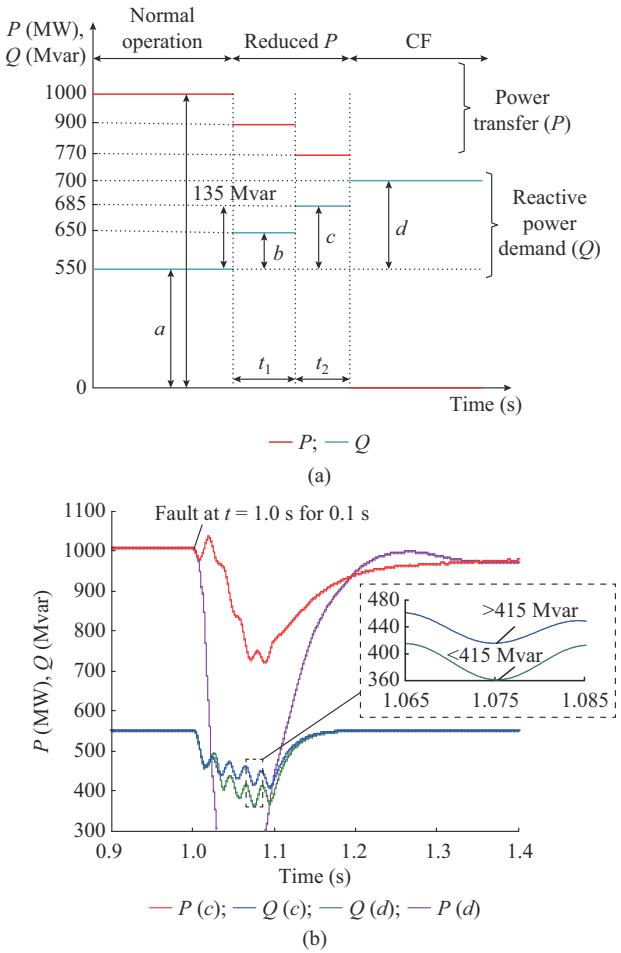

Fig. 2. CIGRE reactive power. (a) Support required. (b) Without support.

Similarly, the CIGRE benchmark model with SCR of 3.0 and 5.0 has CFII of 16.8% and 30.1%, respectively. Since the SCR of the remote converter is set to be 5.0, it can sustain a fault up to 301 Mvar. Or, the remote converter can support local converter with a maximum of 301 Mvar reactive power without CF in multi-infeed scenario. This will help understand the influence of remote converter on local converter under local CF.

B. Multi-infeed System

The 1000 MW 500 kV CIGRE HVDC first benchmark model is adopted as reference to introduce the phenomenon [21]. Figure 3 shows a simplified schematic diagram of dual-infeed scenario used in this paper. Both inverters have reactive power support from installed filters and static capacitors cumulatively labelled as Q_{c1} and Q_{c2}, respectively. Each AC system to which the $HVDC_1$ and $HVDC_2$ are connected is represented by equivalent Thevenin voltage sources (E_1, E_2) and the corresponding impedances (Z_{s1}, Z_{s2}). The voltages of converter bus at the receiving-end (U_1, U_2) are set to be 230 kV during normal operation. Both the inverter-side commutation buses are connected to each other via a 1000 MVA 50 Hz 230 kV/230 kV coupling transformer with Y-Y connection. In practice, the commutation buses are normally connected by the transmission line Z_{tie} instead of the coupling transformer. The coupling transformer here is only to pro-

vide an easier way to obtain the desired MIIF. θ_1 and θ_2 are the receiving-end AC phase angles; ϕ_1 and ϕ_2 are the receiving-end AC source angles; T_1 and T_2 are the transformer ratios of rectifiers 1 and 2, respectively; X_{T1} and X_{T2} are the saturation reactances of transformers at inverters 1 and 2, respectively; γ_1 and γ_2 are the firing angles of inverters 1 and 2, respectively; U_{d1}, I_{d1}, U_{d2}, I_{d2} are the DC voltages and currents of inverters 1 and 2, respectively; P_{d1}, Q_{d1}, P_{d2}, Q_{d2} are the active and reactive power supplied by inverters 1 and 2, respectively; δ_1 and δ_2 are the AC voltage angles of inverters 1 and 2, respectively; P_{12} and Q_{12} are the active and reactive power transfer between commutating buses of inverters 1 and 2, respectively; X_t is the reactance of transformer; and L_f is the inductance of fault.

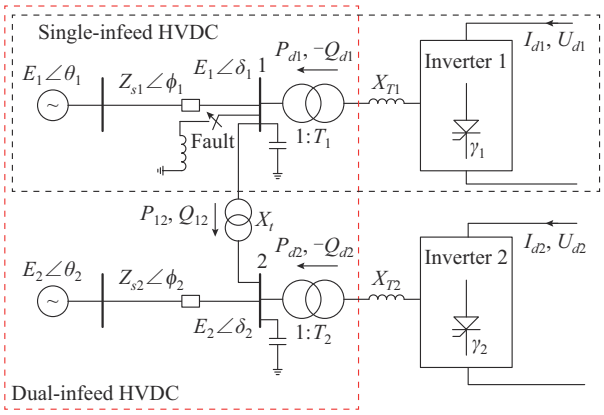

Fig. 3. Multi-infeed HVDC configuration.

For general assumption, inverter 1 is taken as the local converter, while inverter 2 is considered as the remote converter. Here, only three-phase balanced inductive fault is considered.

In single-infeed HVDC, $MIIF = 0$, which means the nearby remote converter does not have influence on the local converter. This is the ideal case, but practically, it can be assumed that if $MIIF \le 0.15$, both converters are working as single-infeed, and the remote converter will not be affected by local faults [3]. On the other hand, if $0.15 < MIIF \le 0.4$, moderate interaction will be observed for both converters. If $MIIF > 0.4$, there is a strong interaction between converters [3].

The positive sequence leakage reactance of coupling transformer (X_t in Fig. 3) is varied to obtain the MIIF used in this paper, as shown in Fig. 4.

C. Multi-infeed CF Configuration

To investigate the influence of MIIF on local CF and concurrent CF, only the strength and MIIF of local AC system is varied, while all other parameters are kept constant. The SCR_2 of remote system is set to be 5.0 and no additional reactive power support is provided in cases 1-3 below.

1) Case 1: C-CFII with Blocked Local Converter

In this case, the local converter is permanently blocked to investigate the behavior of the network on remote CF. Only local converter is disconnected from service, while the local AC system, coupling transformer and complete remote HVDC system will continue their operations.

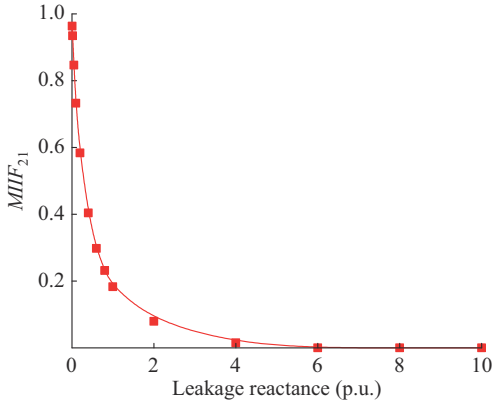

Fig. 4. $MIIF_{21}$ v.s. leakage reactance of transformer.

The MIIF between two systems is set to be 0.492 with $X_t = 0.3$ p.u., while $SCR_1 = 2.5$. Various faults are then applied at the local converter bus, and the CF of remote converter is observed. As local converter is disconnected, there would be no severe interaction between converters. Figure 5 shows the increased remote CFII, i.e., 70%, when the local converter is out of service. The probability of remote CF increases as the fault greater than 70% is applied at local bus, and it becomes 1 with around 83% fault severity.

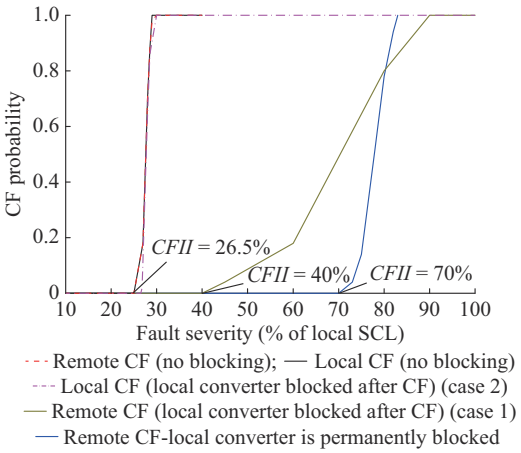

Fig. 5. Local CF and concurrent CF (local converter is permanent disconnected/disconnected after local CF) with $SCR_1 = 2.5$, $SCR_2 = 5$, $Z_{12} = 0.3$, $MIIF_{21} = 0.492$.

2) Case 2: C-CFII with Post Local CF Converter Blockage

In the CIGRE benchmark model, constant extinction angle (CEA) control is implemented at the inverter side, which is not intelligent enough to increase γ on detection of CF. However, practically, a controller has the ability to detect CF and take remedial steps in order to prevent further energy loss. In order to study the behavior of such scenarios, local converter is intentionally blocked after detecting the CF. This way, the post CF inter-converter interaction can be avoided. The concurrent CF probability is shown in Fig. 5 (case 2) with CFII of 40%. The results show that for case 2, the faults severer than 40% of local SCL may cause CF, and that the probability of CF becomes 1 at 90% fault severity. The reduction of CFII from 70% to 40% clearly explains that the operation of both inverters drops the C-CFII even in

case 2. The other most important observation is that the L-CFII is improved with the presence of second converter in proximity with an MIIF of 0.492. Initially, the CFII for single-infeed HVDC system ($MIIF=0$) was 13.5%, but now the L-CFII is almost 26.5%, as shown in Fig. 5. This phenomenon is discussed in the following section with more details of how the local and C-CFII are being influenced by MIIF.

3) Case 3: Multi-infeed CF Analysis Without Converter Blockage

This case is more practical and worse. Suppose there is no such system to block a converter after CF. All converters in close proximity will observe post CF interaction that will deteriorate the voltage profile at converter bus, and consequently, the probability of concurrent CF increases. The probabilities of local CF and concurrent CF are given in Fig. 6 for a wide range of MIIF and local AC system strength.

It is quite clear from the results that the local L-CFII and C-CFII are, as expected, improved with the increase of AC system strength. The other interesting results are about the influence of MIIF on local and C-CFII. With the increase of MIIF, the L-CFII is increased from 18% to 40% while the C-CFII is reduced from 100% to 41% provided $SCR_1=2.5$ and $SCR_2=5.0$. Similarly, for $SCR_1=3.0$ and $SCR_2=5.0$, the L-CFII is increased from 21.5% to 45%, and the C-CFII is reduced from 100% to 46%. And for $SCR_1=5.0$ and $SCR_2=5.0$, the L-CFII is increased from 35% to 50%, and the C-CFII is reduced from 100% to 60%. This increase of L-CFII is due to the ability of inverter to operate under reduced reactive power. As discussed before, the inverter can sustain a fault which does not cause a drop in reactive power greater than 301 Mvar (with $SCR=5.0$, $P=1000$ MW). Thus, the remote inverter can support local inverter up to 301 Mvar depending on MIIF via the inter-connection link. The ability of remote inverter to support local inverter depends on MIIF and available reactive power. Higher value of MIIF gives an easier way to support the local inverter. Table I explains the impact of MIIF on local and C-CFII.

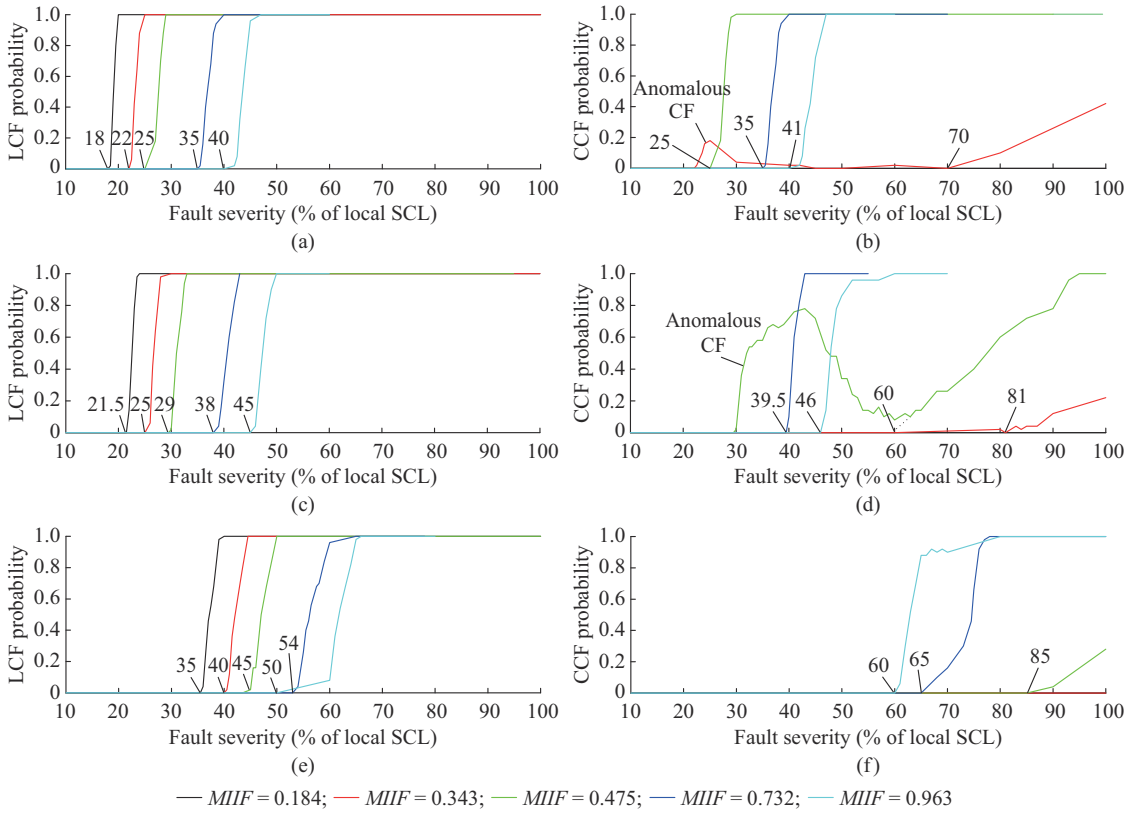

Fig. 6. Local and concurrent CF (without converter blocking) with $SCR_2=5.0$. (a) LCF probability with $SCR_1=2.5$. (b) CCF probability with $SCR_1=2.5$. (c) LCF probability with $SCR_1=3.0$. (d) CCF probability with $SCR_1=3.0$. (e) LCF probability with $SCR_1=5.0$. (f) CCF probability with $SCR_1=5.0$.

It should be noticed that the higher value of MIIF reduces the C-CFII, but at the same time, increases the L-CFII as explained in Fig. 6, where LCF and CCF represent the local CF and concurrent CF, respectively.

D. Role of MIIF in L-CFII

In [10], it is analyzed that MIIF only influences the C-CFII (not L-CFII) of multi-infeed systems including all inverters. This is true because as MIIF increases, the electrical connectivity between converters increases, and local fault appears to influence the remote converter in the same way as it influences the local converter. But the results obtained in this paper is contrary to what is investigated in [10]. It is found that MIIF not only affects C-CFII but also affects L-CFII as shown in Fig. 7. The aforementioned results clearly explain that to some extent, the voltage profile at local converter is being improved via the inter-connection link between converters. When a local fault occurs, the voltage at local commutation bus is reduced, and the reactive power

support flows from remote converter to local converter, which reduces the possibility of local CF. The voltage at remote bus is also reduced, but this depends on MIIF.

In the CIGRE benchmark model ($SCR = 5.0$, $P = 1000$ MW), the remote converter can supply a reactive power support of 301 Mvar without any additional reactive power device (case 3). If the remote converter has some additional reactive power support, then it can supply more power to the local converter during fault.

Moreover, if the local converter is blocked after the CF, then the remote CFII increases (case 2). The reactive power flow from remote converter to local converter (Q_{21}) is shown in Fig. 8 with the local fault severity of 25%, 30%, and 40%, respectively. The bigger value of $MIIF_{21}$ allows more reactive power to flow, which supports the voltage profile of local bus and results in higher L-CFII.

TABLE I
INFLUENCE OF MIIF ON LOCAL CF AND CONCURRENT CF

Without additional reactive power support					With 300 Mvar static synchronous compensator (STATCOM) at remote inverter 2				
SCR_1	SCR_2	$MIIF_{21}$	L-CFII (%)	C-CFII (%)	SCR_1	SCR_2	$MIIF_{21}$	L-CFII (%)	C-CFII (%)
2.5	5.0	0.223	18.0	100.0	2.5	5.0	0.223	38	100
2.5	5.0	0.366	22.0	70.0	2.5	5.0	0.366	40	94
2.5	5.0	0.492	25.0	25.0	2.5	5.0	0.492	46	67
2.5	5.0	0.751	35.0	35.0	2.5	5.0	0.751	54	69
2.5	5.0	0.967	40.0	41.0	2.5	5.0	0.967	62	62
3.0	5.0	0.216	21.5	100.0	3.0	5.0	0.216	44	100
3.0	5.0	0.365	25.0	81.0	3.0	5.0	0.365	48	100
3.0	5.0	0.497	29.0	60.0	3.0	5.0	0.497	52	92
3.0	5.0	0.744	38.0	39.5	3.0	5.0	0.744	60	73
3.0	5.0	0.964	45.0	46.0	3.0	5.0	0.964	67	77
5.0	5.0	0.184	35.0	100.0	5.0	5.0	0.184	60	100
5.0	5.0	0.343	40.0	100.0	5.0	5.0	0.343	66	100
5.0	5.0	0.475	45.0	85.0	5.0	5.0	0.475	68	94
5.0	5.0	0.732	54.0	65.0	5.0	5.0	0.732	78	91
5.0	5.0	0.963	50.0	60.0	5.0	5.0	0.963	84	89

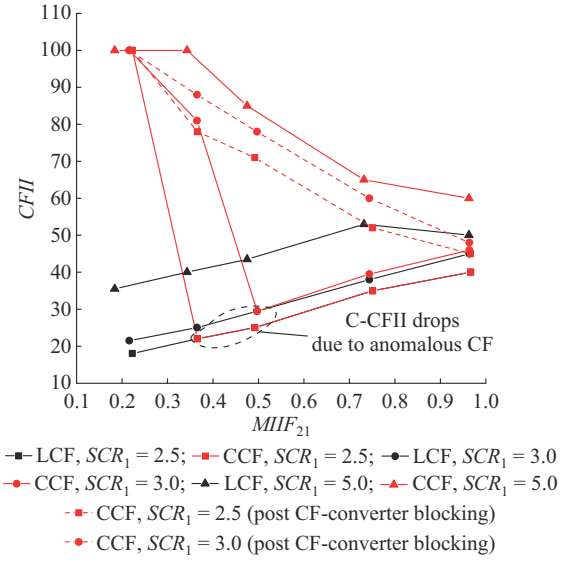

Fig. 7. Behavior of L-CFII and C-CFII w.r.t. $MIIF_{21}$ (case 3) with $SCR_2 = 5.0$ without post fault converter blocking.

E. The Maximum Limit of MIIF

It is true that MIIF influences both the L-CFII and C-CFII; bigger value of MIIF increases the L-CFII while reducing the C-CFII. Thus, there must be a reasonable MIIF which can support L-CFII without letting down the C-CFII too much in case that the remote converter becomes more vulnerable to minor faults. If the post local CF converter blocking scheme is used, the remote converter may have higher CFII even with increased MIIF. Figures 6 and 7 show that there is a tradeoff between the L-CFII and C-CFII, which means that both should be above the minimum level based on both the configuration of converter station and associated AC system.

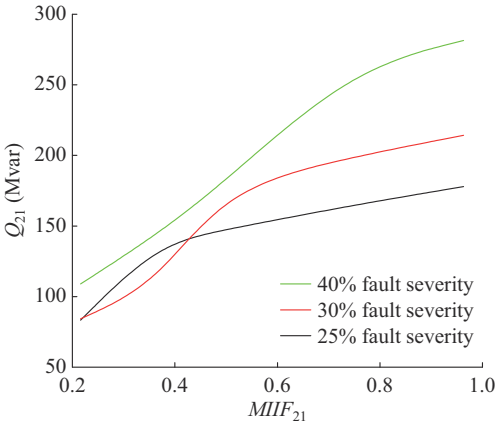

Fig. 8. Q_{21} flow w.r.t. $MIIF_{21}$ (case 3, Fig. 6(b)).

F. Anomalous CF

Anomalous CF basically occurs due to voltage distortion

because of the harmonic contents in AC commutation bus voltage [10]. A less severe fault may advance the zero crossing of commutation voltage due to poor quality of voltage wave, which ultimately reduces the voltage-time area. Consequently, the CF probability increases. However, this does not happen for all AC system strengths and MIIF. The chances of anomalous CF for MIIF less than 0.3 or greater than 0.5 are quite rare and even zero. The anomalous CF can also be reduced if the post local CF converter is blocked or additional reactive power support is provided at the remote end. In Fig. 7, the dashed lines show C-CFII when the local converter is blocked after CF, where a significant increase in CFII can be observed.

IV. Mathematical Modeling of Power Flow

The measured value of $MIIF_{21}$ over coupling reactance X_t between converters is shown in Fig. 4. In order to model the reactive power flow between commutation buses, a mathematical relation of $MIIF_{21}$ and X_t is required. Heuristically, $MIIF_{21}$ seems to be an exponential function. Various exponential functions relating X_t and $MIIF_{21}$ are shown in Fig. 9. The error between the mathematical function and measured value is also plotted.

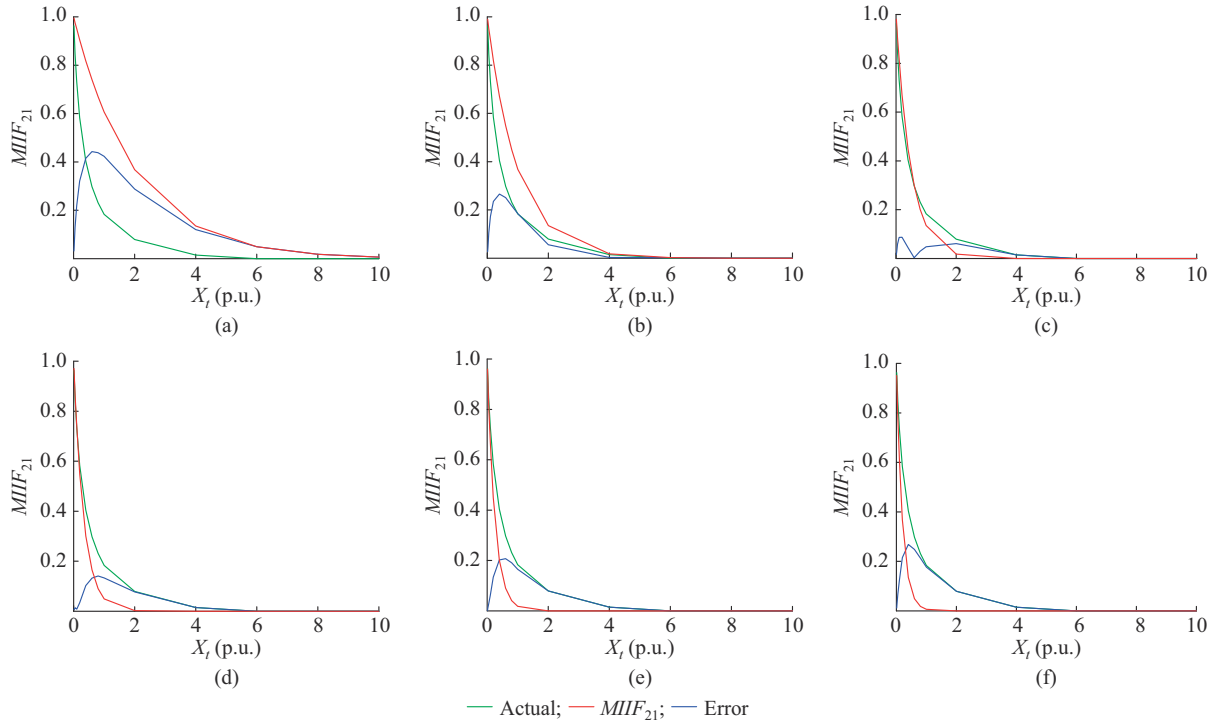

Fig. 9. Relations of $MIIF_{21}$ and X_t. (a) $MIIF_{21}=e^{-0.5X_t}$. (b) $MIIF_{21}=e^{-X_t}$. (c) $MIIF_{21}=e^{-2X_t}$. (d) $MIIF_{21}=e^{-3X_t}$. (e) $MIIF_{21}=e^{-4X_t}$. (f) $MIIF_{21}=e^{-5X_t}$.

Intuitively, the best approximation can be expressed by (5) as illustrated in Fig. 10. Equation (5) is actually the average of all functions in Fig. 9, which results in the minimum error; therefore, it is adopted in the modeling of Q_{21}. The reactive power flow between two buses can be calculated as (7). If we assume $\cos(\delta_2-\delta_1)=1$, then (7) is simplified as (8).

$$X_t=\frac{1}{6}\left(\frac{1}{0.5}\ln\left(\frac{1}{MIIF_{21}}\right)+\sum_{n=1}^{5}\frac{1}{n}\ln\left(\frac{1}{MIIF_{21}}\right)\right) \tag{5}$$

$$X_t=0.7139\ln\left(\frac{1}{MIIF_{21}}\right) \tag{6}$$

$$Q_{21}=\frac{V_2V_1}{X_t}\cos(\delta_2-\delta_1)-\frac{V_1^2}{X_t} \tag{7}$$

$$Q_{21}=\frac{V_1(V_2-V_1)}{X_t} \tag{8}$$

where V_1, V_2, and X_t are the voltage magnitudes of buses of converter 1 and 2, and the reactance between these two buses, respectively.

Substituting (6) to (8), we can obtain:

$$Q_{21}=\frac{V_1\Delta V_{21}}{0.7139\ln\left(\frac{1}{MIIF_{21}}\right)} \tag{9}$$

where $\Delta V_{21}=V_2-V_1$.

Equation (9) describes a relation between $MIIF_{21}$ and Q_{21}. As the remote converter supports local converter by providing a reactive power compensation during faulty conditions, the CFII at local converter ($LCFII_{21}$) will increase and can be calculated as:

$$LCFII_{21}=CFII_1+CFII_{21} \tag{10}$$

$$CFII_{21}=\frac{Q_{21}}{P_{dc}}\times 100 \tag{11}$$

where $CFII_{21}$ is the increase in $LCFII_{21}$ due to the support of remote-end converter.

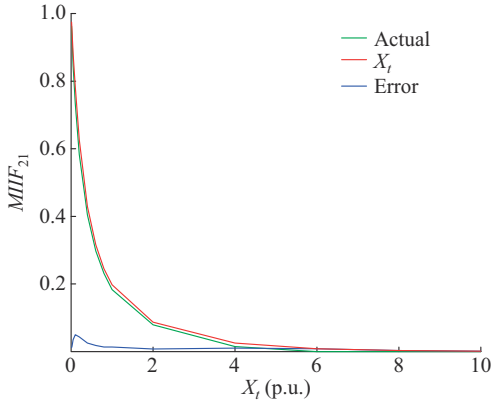

Fig. 10. Optimal function relating $MIIF_{21}$ and X_t.

V. Verification

In order to verify (9), a dual-infeed HVDC simulation setup is built in PSCAD/EMTDC as in Fig. 3. A constant fault of 150 Mvar is applied at $t_s = 1.0$ s at the bus of local converter 1, and removed at $t_e = 1.1$ s. The case with AC system strength of $SCR_1 = 2.5$ and $SCR_2 = 5.0$ is considered. The flow of reactive power Q_{21} is measured and shown in Fig. 11 along with the calculated value. The graphical results in Fig. 11 explain the validity of approximation. It is to mention that Q_{21} also depends on fault severity as illustrated in Fig. 12. The severe fault causes more reactive power to flow because it produces big ΔV_{21}.

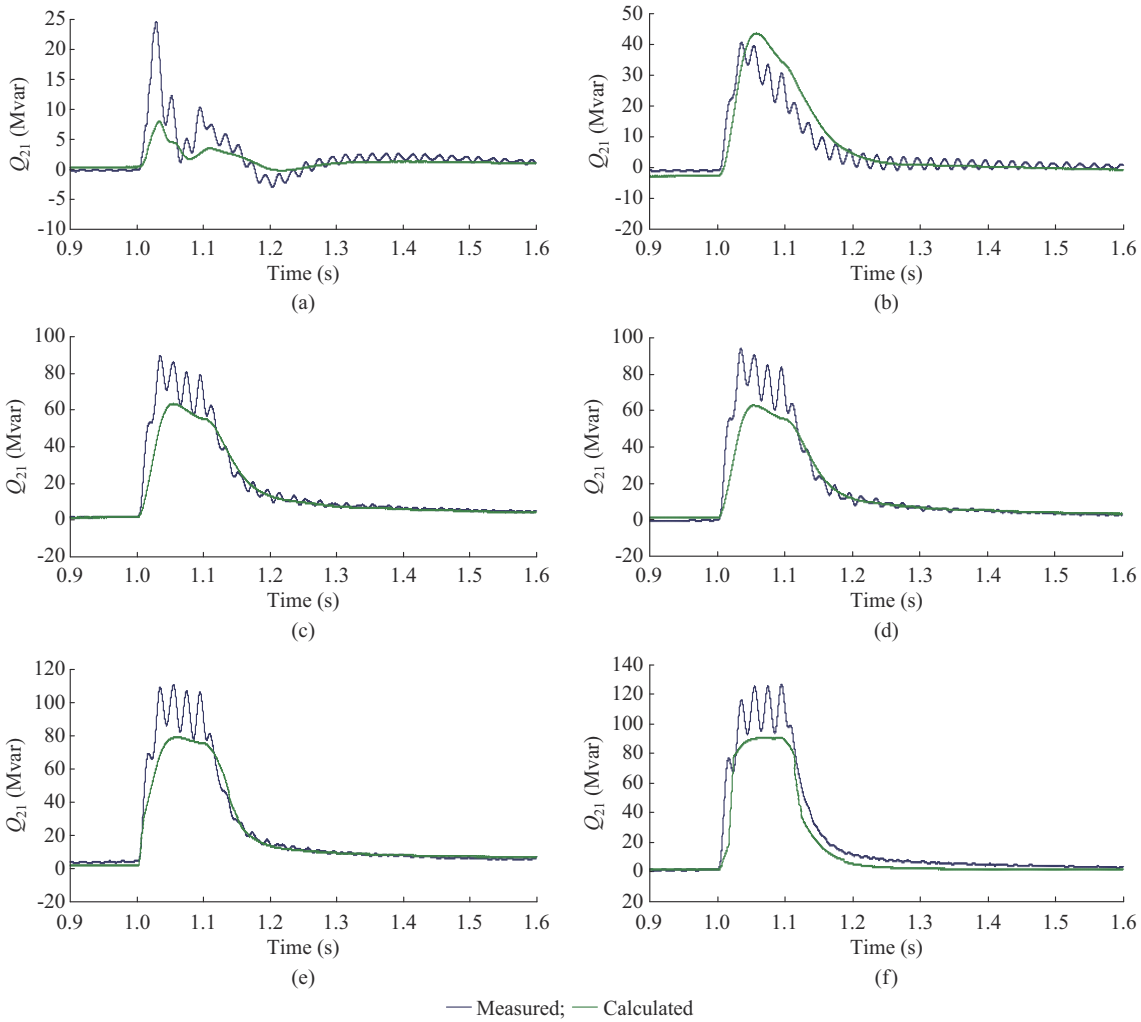

Fig. 11. Q_{21} approximation for $SCR_1 = 2.5$ and $SCR_2 = 5.0$ with $P_1 = 1000$ MW, $P_2 = 1000$ MW, $t_s = 1.0$ s, and $t_e = 1.1$ s. (a) $X_t = 6$ p.u., $MIIF_{21} < 0.015000$. (b) $X_t = 4$ p.u., $MIIF_{21} = 0.015095$. (c) $X_t = 4$ p.u., $MIIF_{21} = 0.183407$. (d) $X_t = 6$ p.u., $MIIF_{21} = 0.231819$. (e) $X_t = 0.4$ p.u., $MIIF_{21} = 0.404145$. (f) $X_t = 0.1$ p.u., $MIIF_{21} = 0.732026$.

To verify (10), the dual-infeed HVDC system is investigated for three cases, i.e., ① $SCR_1 = 2.5$, $SCR_2 = 5.0$; ② $SCR_1 = 3.0$, $SCR_2 = 5.0$; and ③ $SCR_1 = 5.0$, $SCR_2 = 5.0$. The measured values of L-CFII using electromagnetic transient simulations and the calculated values using (10) are provided in Table II.

The aforementioned results clearly explain that the L-CFII has an influence of $MIIF_{21}$ in multi-infeed HVDC configuration. It is evident from the tabulated and graphical results that the L-CFII increases with the increase of $MIIF_{21}$. The reactive power support Q_{21} is observed over various $MIIF_{21}$, which yields bigger L-CFII. Initially, the L-CFII for $MIIF_{21} = 0$ is 13.5%, 16.8%, and 30.1% of SCL for cases 1, 2, and 3, respectively. However, the flow of Q_{21} reduces the possibili-

ty of local CF, and results in bigger L-CFII as shown in Table II. The error is caused due to the approximation of Q_{21}, and is acceptable and adequately validates the presented theory.

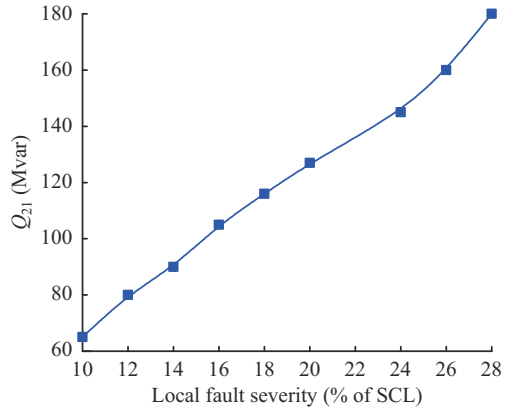

Fig. 12. Q_{21} v.s. fault severity.

VI. Conclusion

This paper provides a detailed analysis of local CF and concurrent CF in multi-infeed HVDC system. The impact of MIIF on local CF in inverter-inverter multi-infeed case is probed deeply. It has been investigated that both the local and concurrent CF depend on MIIF. It is proven that the converters in LCC-HVDC system can work under reduced reactive power as per CFII. The bigger the CFII is, the more reactive power a converter can provide without CF. This provides a reactive power support via interconnection link to local converter in case of local faults. The bigger value of MIIF provides a stronger path between commutation buses of multi-infeed scenario. The flow of reactive power support from remote converter to local converter improves the voltage profile of local converter bus, and consequently, the probability of local CF is reduced. It is true that bigger value of MIIF increases the probability of concurrent CF and leads to less C-CFII, but at the same time, it decreases the probability of local CF leading to bigger L-CFII. The CIGRE benchmark model with SCR of 2.5, 3.0, and 5.0 has the ability to provide a maximum reactive power support of 135 Mvar, 168 Mvar, and 301 Mvar, respectively, to local converter without facing a CF, which improves the L-CFII. Furthermore, if the remote converter has any additional reactive power support, it can further strengthen the L-CFII. A mathematical model of the increase in L-CFII in multi-infeed HVDC system is provided. A few case studies are investigated in order to prove mathematically the theory presented. A relation describing MIIF and reactive power flow between commutation buses is formulated. Therefore, the statement that the local CF is independent of MIIF need to be revised. The results are verified by EMT simulations in PSCAD/EMTDC.

Thus, for practical projects, it is very much essential to maintain the MIIF to a certain level for optimal value of CFII for all converters in proximity.

TABLE II
Increase in L-CFII for Multi-infeed HVDC Configuration

SCR_1	SCR_2	X_t (p.u.)	$MIIF_{21}$	Maximum Q_{21} (measured) (Mvar)	Local worst power (calculated) (Mvar)	L-CFII (calculated) (% of SCL)	L-CFII (measured) (% of SCL)	Error (% of SCL)	Increase in L-CFII (% of SCL)
		0.01	0.966825	250	385	38.5	40.0	1.5	26.5
		0.10	0.750943	220	355	35.5	35.0	0.5	21.5
2.5	5	0.30	0.491573	150	285	28.5	25.0	3.5	11.5
		0.50	0.365854	120	255	25.5	22.0	3.5	8.5
		1.00	0.222591	80	215	21.5	18.0	3.5	4.5
		0.01	0.966825	275	443	44.3	45.0	0.7	28.2
		0.10	0.750943	242	410	41.0	38.0	3.0	21.2
3.0	5	0.30	0.491573	160	328	32.8	29.5	3.3	12.7
		0.50	0.365854	110	278	27.8	25.0	2.8	8.2
		1.00	0.222591	83	251	25.1	21.5	3.6	4.7
		0.01	0.966825	245	546	54.6	50.0	4.6	19.9
		0.10	0.750943	240	541	54.1	53.0	1.1	22.9
5.0	5	0.30	0.491573	172	473	47.3	43.5	3.8	13.4
		0.50	0.365854	135	436	43.6	40.0	3.6	9.9
		1.00	0.222591	85	386	38.6	35.5	3.1	5.4

References

[1] B. Rehman and C. Liu, "AC/DC multi-infeed power flow solution," *IET Generation, Transmission & Distribution*, vol. 13, no. 10, pp. 1838-1844, Apr. 2019.

[2] Y. Shao and Y. Tang, "Fast evaluation of commutation failure risk in multi-infeed HVDC systems," *IEEE Transactions on Power Systems*, vol. 33, no. 1, pp. 646-653, Jan. 2018.

[3] D. K. B. Davies, A. Williamson, A. M. Gole *et al*., "Systems with multiple DC infeed," *Cigré Publication 364 (WG B4.41)*, pp. 1-118, Aug. 2008.

[4] S. Mirsaeidi, X. Dong, D. Tzelepis *et al*., "A predictive control strategy for mitigation of commutation failure in LCC-based HVDC systems," *IEEE Transactions on Power Electronics*, vol. 34, no. 1, pp. 160-172, Jan. 2019.

[5] E. Rahimi, A. M. Gole, J. B. Davies *et al*., "Commutation failure in single- and multi-infeed HVDC systems," in *Proceedings of IEEE International Conference on AC and DC Power Transmission*, London,

UK, Mar. 2006, pp. 182-186.
[6] Y. Zhou, H. Wu, W. Wei *et al*., "Optimal allocation of dynamic var sources for reducing the probability of commutation failure occurrence in the receiving-end systems," *IEEE Transactions on Power Delivery*, vol. 34, no. 1, pp. 324-333, Feb. 2019.
[7] H. Xiao and Y. Li, "Multi-infeed voltage interaction factor: a unified measure of inter-inverter interactions in hybrid multi-infeed HVDC systems," *IEEE Transactions on Power Delivery*, vol. 35, no. 4, pp. 2040-2048, Aug. 2020.
[8] H. Xiao, Y. Li, J. Zhu *et al*., "Efficient approach to quantify commutation failure immunity levels in multi-infeed HVDC systems," *IET Generation, Transmission & Distribution*, vol. 10, no. 4, pp. 1032-1038, Mar. 2016.
[9] Z. Wei, J. Liu, W. Fang *et al.*, "Commutation failure analysis in single- and multi-infeed HVDC systems," in *Proceedings of IEEE PES Asia-Pacific Power and Energy Engineering Conference (APPEEC)*, Xi'an, China, Oct. 2016, pp. 2244-2249.
[10] E. Rahimi, A. M. Gole, J. B. Davies *et al*., "Commutation failure analysis in multi-infeed HVDC systems," *IEEE Transactions on Power Delivery*, vol. 26, no. 1, pp. 378-384, Jan. 2011.
[11] C. Zhou and Z. Xu, "Study on commutation failure of multi-infeed HVDC system," in *Proceedings of International Conference on Power System Technology*, Kunming, China, Oct. 2002, pp. 2462-2466.
[12] X. Chen, A. M. Gole, and M. Han, "Analysis of mixed inverter/rectifier multi-infeed HVDC systems," *IEEE Transactions on Power Delivery*, vol. 27, no. 3, pp. 1565-1573, Jul. 2012.
[13] F. Wang, T. Liu, and X. Li, "Decreasing the frequency of HVDC commutation failures caused by harmonics," *IET Power Electronics*, vol. 10, no. 2, pp. 215-221, Feb. 2017.
[14] C. Guo, Y. Liu, C. Zhao *et al*., "Power component fault detection method and improved current order limiter control for commutation failure mitigation in HVDC," *IEEE Transactions on Power Delivery*, vol. 30, no. 3, pp. 1585-1593, Jun. 2015.
[15] C. V. Thio, J. B. Davies, and K. L. Kent, "Commutation failures in HVDC transmission systems," *IEEE Transactions on Power Delivery*, vol. 11, no. 2, pp. 946-953, Apr. 1996.
[16] W. Yao, C. Liu, J. Fang *et al*., "Probabilistic analysis of commutation failure in LCC-HVDC system considering the CFPREV and the initial fault voltage angle," *IEEE Transactions on Power Delivery*, vol. 35, no. 2, pp. 715-724, Apr. 2020.
[17] Q. I. Wang, C. Zhang, X. Wu *et al*., "Commutation failure prediction method considering commutation voltage distortion and DC current variation," *IEEE Access*, vol. 7, pp. 96531-96539, Jul. 2019.
[18] E. Rahimi, S. Filizadeh, and A. Gole, "Commutation failure analysis in HVDC systems using advanced multiple-run method," in *Proceedings of International Conference on Power Systems Transients*, Montreal, Canada, Jun. 2005, pp. 1-5.
[19] C. Guo, Y. Zhang, A. M. Gole *et al.*, "Analysis of dual-infeed HVDC with LCC-HVDC and VSC-HVDC," *IEEE Transactions on Power Delivery*, vol. 27, no. 3, pp. 1529-1537, Jul. 2012.
[20] *IEEE Guide for Planning DC Links Terminating at AC Locations Having Low Short-circuit Capacities*, IEEE Working Group 15.05.05, 1997.
[21] M. Szechtman, T. Wess, and C. V. Thio, "A benchmark model for HVDC system studies," in *Proceedings of International Conference on AC and DC Power Transmission*, London, UK, Sept. 1991, pp. 374-378.

Bilawal Rehman received the B.S. and M.S. degrees in electrical engineering from University of Management & Technology, Lahore, Pakistan, in 2012 and 2015, respectively. He has completed Ph.D. degree in power system & automation in the School of Electrical and Electronic Engineering, North China Electric Power University, Beijing, China, in 2020. His current research interests include operation and control of multi-infeed HVDC system, hybrid LCC-VSC HVDC, and AC/DC power flow.

Chongru Liu received her B.E., M.S., and Ph.D. degrees in electrical engineering from Tsinghua University, Beijing, China. She was a Visiting Professor at the University of Hong Kong, Hong Kong, China, from 2009 to 2010, and at Washington State University, Pullman, USA, from 2010 to 2011. She is currently a Professor in the School of Electrical and Electronic Engineering, North China Electric Power University, Beijing, China. She is a Member of the National Power System Management and Information Exchange Standardization Committee of China. She is a member of Beijing Nova and supported by the program of New Century Excellent Talents in University. Her current research interests include HVDC system control and simulation, and control, operation, and simulation of MMC-VSC system.

Huan Li received the B.S. degree in electrical and electronic engineering from Huazhong University of Science and Technology, Wuhan, China, in 2008, and the Ph.D. degree in power system and its automation from Huazhong University of Science and Technology, Wuhan, China, in 2014. He has been with the Electric Power Research Institute, China Southern Power Grid since 2014. His current research interests include power protection, transient stability and HVDC.

Chuang Fu received the B.S. degree in hydro-electrical engineering from Sichuan Institute of Technology, Chengdu, China, in 1996, and the M.S. and Ph.D. degrees in electrical engineering from Huazhong University of Science and Technology, Wuhan, China, in 1999 and 2003, respectively. He has been with the Electric Power Research Institute, China Southern Power Grid since 2005. His current research interests include HVDC and protection and control of power systems.

Wei Wei received the B.S. and the M.S. degrees in power system and its automation from North China Electric Power University, Baoding, China, in 2002 and 2005, respectively. He has been with the Electric Power Research Institute, China Southern Power Grid since 2012. His current research interests include power protection, transient stability and HVDC.